Quantum criticality at the origin of life

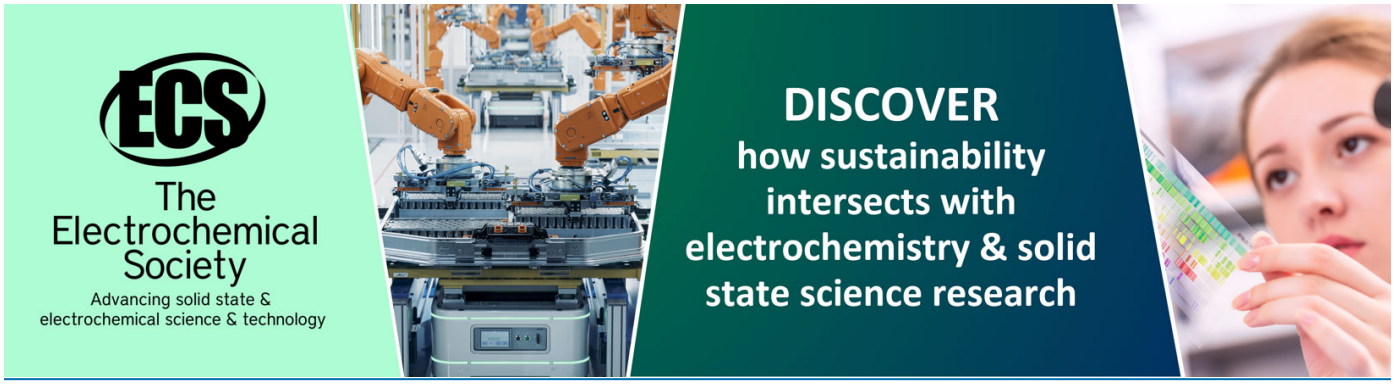

Journal of Physics: Conference Series **626** (2015) 012023 doi:10.1088/1742-6596/626/1/012023

Quantum criticality at the origin of life

Gábor Vattay[1], Dennis Salahub[2], István Csabai[1], Ali Nassimi[2,3] and Stuart A Kaufmann[2,4]

[1] Department of Physics of Complex Systems, Eötvös University, 1117 Budapest, Pázmány P. s. 1/A, Hungary

[2]Department of Chemistry, CMS - Centre for Molecular Simulation and IQST - Institute for Quantum Science and Technology, University of Calgary, 2500 University Drive NW, Calgary, Alberta, Canada T2N 1N4

[3] Chemical Physics Theory Group, Department of Chemistry, University of Toronto, 80 Saint George Street, Toronto, ON M5S 3H6, Canada

[4] Institute for Systems Biology, Seattle, WA 98109, USA

E-mail: vattay@elte.hu

Abstract. Why life persists at the edge of chaos is a question at the very heart of evolution. Here we show that molecules taking part in biochemical processes from small molecules to proteins are critical quantum mechanically. Electronic Hamiltonians of biomolecules are tuned exactly to the critical point of the metal-insulator transition separating the Anderson localized insulator phase from the conducting disordered metal phase. Using tools from Random Matrix Theory we confirm that the energy level statistics of these biomolecules show the universal transitional distribution of the metal-insulator critical point and the wave functions are multifractals in accordance with the theory of Anderson transitions. The findings point to the existence of a universal mechanism of charge transport in living matter. The revealed bio-conductor material is neither a metal nor an insulator but a new quantum critical material which can exist only in highly evolved systems and has unique material properties.

Advances in the theory of complex systems over the last quarter century reinforced that living systems exist at the edge of chaos[1, 2, 3, 4] and order, poised at criticality[5]. Finding the detailed mechanism behind this apparent self-organized criticality[6, 7] is still a tantalizing problem. One of the fascinating aspects of life is the highly organized molecular machinery taking care of myriads of complex processes such as DNA replication, protein synthesis, cell division and metabolism, to mention only a few. Electric forces animating the parts require a perpetual and precise motion of charges throughout the system for perfect execution of biochemical tasks. In this paper we show that practically all biomolecules, from small signalling molecules to proteins taking part in biochemical electronic processes, belong to a fundamentally new class of conducting material. This is a disordered conductor where the strength of the disorder is tuned exactly to the metal-insulator transition point and it is consequently in a permanent critical quantum state.

Our initial perspective is that of condensed-matter physics. The unique properties of the critical quantum state at the localization-delocalization transition point have been described first in the the well known Anderson[8] model, which represents the current paradigm for understanding conduction in condensed matter. In the Anderson Hamiltonian $H = \sum_j \epsilon_i a_i^+ a_i - \sum_{<ij>} a_j^+ a_i$ on a 3D lattice with random uniformly distributed on-site energies $\epsilon_i \in [-W, W]$, the critical level of disorder[9] is $W_c = 16 \pm 0.5$. For $W < W_c$ the system is a disordered

metal with extended states and for $W > W_c$ the states are localized and the system is an insulator. It has been shown[10] that in the exact critical point of the Anderson transition ($W = W_c$) the electron eigenfunctions are extended, but strongly inhomogeneous multifractals[11]. Similar metal-insulator transitions (MIT) exist in a wide range of physical systems at various dimensionalities[12] including the 1D Harper-Hofstadter model[13] and quantum-Hall-type transitions.

For example, the 1D Harper model[14] describes the energy spectrum of an electron in a 2D lattice, whose graphic representation is widely known as the Hofstadter butterfly[13]. In the related Aubry-André Hamiltonian[15] $H = \sum_j \lambda \cos(2\pi\sigma i) a_i^+ a_i - \sum_{<ij>} a_j^+ a_i$, where $\sigma = (\sqrt{5}-1)/2)$ is the Golden Mean Ratio, the critical value separating localized and extended phases is $\lambda_c = 2$. The wave functions are also multifractals[16] there. Other examples include[12] quantum-Hall-type transitions in disordered conductors and superconductors in strong magnetic fields, the spin quantum Hall effect, the thermal quantum Hall effect, Dirac fermions in random vector potentials and Bethe lattices.

MIT-like transitions exist also in low-dimensional quantum chaos. Quantum counterparts of strongly chaotic systems[17] share the properties of delocalized systems, while integrable systems[18] have localized wave functions in quantum numbers corresponding to conserved quantities. Pseudointegrable systems[19] lie at the border of chaos and integrability, where classical trajectories diverge only slowly (with zero Lyapunov exponent) but their dynamics is complex and the periodic orbits proliferate in their phasespace exponentially. Quantized pseudointegrable systems also show all the key features of critical systems, including multifractal wavefunctions[20].

Criticality can also be observed in the energy spectrum of systems at the transition point. Random Matrix Theory[21, 22, 23, 24] (RMT) is the main tool for the characterization of the universal statistical properties of Hamiltonians of complex systems. The distance between consecutive energy levels fluctuates in the spectrum. The raw distance between levels $\sigma_n = E_{n+1} - E_n$ can be normalized using the average separation of levels $\Delta(E)$ at a given energy window around E. The ratio $s_n = \sigma_n/\Delta(E_n)$ is called the level spacing. Random matrix theory has certain predictions for the form of the distribution $P(s)$ of level spacings.

It has been established[25] that in the 3D Anderson model the localized, delocalized and the critical states each have a distinct level spacing distribution. These three distributions are believed to be universal, i.e. independent of the microscopic details of the disordered system. In the delocalized metallic phase ($W < W_c$) the distribution coincides with the level statistics of the Gaussian Orthogonal Ensemble (GOE), which is the ensemble of real symmetric random matrices with identically distributed Gaussian elements. The level spacing distribution is the Wigner surmise[21]

$$P_W(s) = \frac{\pi s}{2} \exp\left(-\frac{\pi s^2}{4}\right).$$

In the localized insulating phase ($W > W_c$) the energy levels form a random Poisson process and the level spacing distribution is exponential

$$P_P(s) = \exp(-s).$$

It has been shown[17, 12, 26] that not only in the 3D Anderson model, but in all other examples of Anderson-like transitions, the energy level statistics in the delocalized phase is universal and corresponds to the proper Gaussian Random Matrix Ensemble reflecting the symmetries of the system, while in the localized phase it is always random Poissonian[18, 12, 26].

At the transitional point ($W = W_c$) a third kind of intermediate spectral statistics $P_T(s)$ exists, which is the hallmark of the critical state[25]. In solid state models theoretical

arguments[27, 28] and numerical studies[29, 30] suggest the general form

$$P_T(s) = c_1 s \exp\left(-c_2 s^{1+\gamma}\right),$$

where c_1 and c_2 are γ dependent normalization constants. In the case of the 3D Anderson model[30] $\gamma \approx 0.2$. In the Harper model[26] and in other pseudointegrable models[31] showing critical quantum chaos a numerical value of $\gamma \approx 0$ has been found[26], which supports the semi-Poissonian distribution

$$P_T(s) = P_{SP}(s) = 4s \exp\left(-2s\right).$$

The semi-Poissonian distribution has also been predicted from a short range plasma model[32] of energy levels introduced in RMT.

While in physical systems the critical state can be reached only upon a careful tuning of the strength of the disorder, in the following we show that certain biomolecules are precisely at the critical state without any external tuning.

The exact numerical solution of the Schrödinger equation for the electronic states of large molecules such as proteins is a prohibitive task. Various approximations have been developed, which reduce the problem to a one-electron problem in the effective field of the remaining electrons. Wave functions of molecules are usually written in the form of Linear Combinations of Atomic Orbitals (LCAO) $\phi_i = \sum_r C_{ir}\chi_r$ where ϕ_i is a Molecular Orbital (MO) represented as the sum of atomic orbital (AO) contributions χ_r. The one-electron eigenenergies and eigenvectors then can be determined from the generalized eigenvalue equation $HC = ESC$, where $S_{rs} = \langle \chi_r \mid \chi_s \rangle$ and $H_{rs} = \langle \chi_r \mid \hat{H}_{eff} \mid \chi_s \rangle$ are the overlap and effective Hamiltonian matrices respectively. The effective Hamiltonian depends on the coefficients which makes the problem nonlinear in C. This is the case in Hartree-Fock and Density Functional Theory (DFT) calculations, which then cannot be routinely carried out for proteins involving thousands of atoms. If we restrict our interest to the localization-delocalization problem in valence electrons and treat the two-electron part of the Hamiltonian as in the case of the electrons in metals, in an average sense only, we can apply semi-empirical methods. Once the positions of the atoms are known the Extended Hückel (EH) Molecular Orbital Method[33] is quite successful in calculating the MOs of organic molecules. The diagonal part $H_{rr}^{(EH)}$ of the EH Hamiltonian is given by the ionization energies of the AOs[34], while the off-diagonal elements are calculated from the diagonal elements and the overlap matrix

$$H_{rs}^{(EH)} = \frac{1}{2} K \left(H_{rr} + H_{ss}\right) S_{rs},$$

where the common choice for the empirical constant is $K = 1.75$. This is similar in spirit to other tight binding Hamiltonians in various models of the Anderson transition.

Myoglobin is the first[35] and one of the best studied protein structures. It plays a central role in the oxygen storage of muscles. It consists of 153 amino acids and weighs about 18000 Daltons. For the numerical studies we selected NMR data of a solution form[36] (PDB ID:1MYF) from the Protein Data Bank[37] of RCSB, as it is captured in the "living" state and contains the positions of hydrogen atoms essential for the calculations. The EH calculations have been carried out by the numerical package YAeHMOP. There are $N = 6329$ valence electron AOs and the EH Hamiltonian and overlap matrices are sufficiently large of dimension 6329×6329, which makes it possible to make a good numerical comparison with similar calculations in solid state physics[16, 30, 25, 24] and quantum chaos[26, 20, 31, 24]. Löwdin transformation of the coefficient vector $C' = S^{1/2}C$ has been applied to transform the EH Hamiltonian to a real symmetric self-adjoint operator $H^L = S^{-1/2}H^{(EH)}S^{-1/2}$, which satisfies a normal eigenequation $H^L C^L = EC^L$.

The Highest Occupied Molecular Orbital (HOMO) and the Lowest Unoccupied Molecular Orbital (LUMO) play a key role both in electron transport and reactions of organic molecules.For the visual demonstration of the fractal nature of the eigenfunctions we show the HOMO and the LUMO of Myoglobin in Fig. 1. Absolute values of coefficients C_r^L are shown such that the index r is ordered in the sequence of appearance of atoms and orbitals in the amino acid sequence of the protein. Statistical similarity of the magnified part of the wave functions to the entire function is a visual indication of a fractal.

The multifractal analysis of the protein wave functions is based on the standard box counting procedure[38], dividing the 1D index space of ordered AO indices along the protein sequence into $N_l \approx N/l$ boxes of size l and determining the box probability of the wave function in the kth box,

$$\mu_k(l) = \sum_{n=0}^{l-1} |C^L_{(k-1)l+n}(E_i)|^2, k = 1, \ldots, N_l,$$

as a suitable measaure. If the qth moments of this measure are counted in all boxes and is proportional to some power $\tau(q)$ of the box size,

$$\chi_q = \left\langle \sum_k \mu_k^q(l) \right\rangle_E \sim l^{\tau(q)},$$

multifractal behaviour might be derived. For a simple monofractal $\tau(q) = (q-1)D$, where D is the fractal dimension. For multifractals the $\tau(q)$ curve is nonlinear and the generalized fractal dimensions D_q can be recovered $\tau(q) = (q-1)D_q = \lim_{L\to 0} \ln \chi_q / \ln l$.

We expect that for extended wave functions in the conducting phase the coefficients are evenly distributed around their mean, which is $\left\langle |C_r^L|^2 \right\rangle_E = (1/N) \sum_{k=1}^N |C_r^L(E_k)|^2 = 1/N$, and are independent of the position due to the normalization of the wave functions. The measure then scales like $\mu_k(l) \sim l/N$ and the moments scale as $\chi_q \sim (l/N)^{(q-1)}$, yielding $D_q = D = 1$ independent of q. For localized states in the insulating phase the coefficients are nearly zero except in a short interval of the size of the localization length ξ. The localization length is much smaller than the system size $\xi \ll N$, therefore at intermediate length scales $\xi \ll l \ll N$ an interval of size l either contains the localization interval and almost the full probability $\mu_k(l) \approx 1$ or it is practically empty $\mu_k(l) \approx 0$. The moments do not scale with the length $\chi_q \sim 1$ and $\tau(q) = 0$ yielding $D_q = D = 0$.

The numerical values of the fractal dimension of the protein wave function can be determined more conveniently by calculating the box probability for all possible boxes of length l and performing an additional averaging to smooth out statistical fluctuations

$$\left\langle \sum_k \mu_k^q(l) \right\rangle_E = N_l \times \frac{1}{N_l} \sum_k \langle \mu_k^q(l) \rangle_E \approx \frac{N}{l} \frac{1}{N-l} \sum_{r=1}^{N-l} \left\langle \left(\sum_{n=1}^{l} |C^L_{r+n}|^2 \right)^q \right\rangle_E .$$

In Fig. 2. we show the generalized fractal dimensions for Myoglobin obtained numerically. The most significant value is the correlation dimension $D_2 \approx 0.5$ which is just midway between localization $D = 0$ and delocalization $D = 1$ confirming that the system is critical and the wave functions are multifractals. We note that the same numerical value $D_2 = 0.5$ has been obtained also for critical quantum chaos[26, 20].

Next we show that the level statistics of Myoglobin is also transitional. The energy levels computed with the EH method have been analyzed with a statistical method of RMT suitable for the analysis of a relatively low number of eigenvalues. The distance between two consecutive levels $\sigma_i = E_{i+1} - E_i$ is normalized with the average of k level spacings to the left and to the right $\Delta_i = \frac{1}{2k+1} \sum_{j=-k}^{j=+k} \sigma_{i+j}$ giving the unfolded level spacing $s_i = \sigma_i/\Delta_i = (2k+1)(E_{i+1} -$

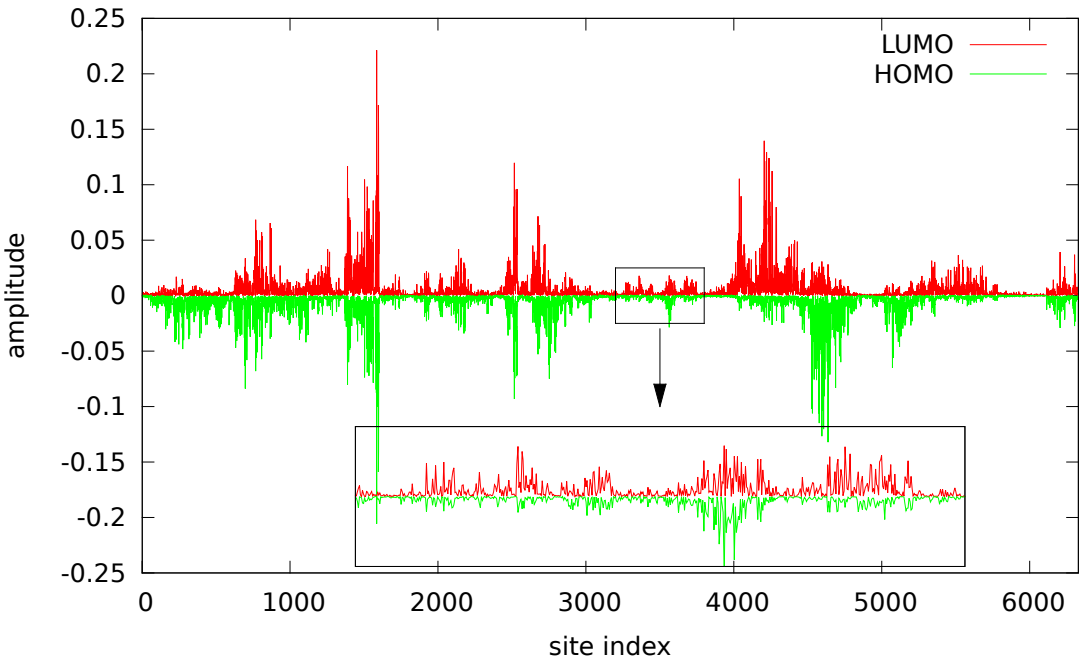

Figure 1. The HOMO/LUMO orbitals for Myoglobin (PDB ID:1MYF) calculated with the Extended Hückel method. Vertical axis: the absolute value of C_r^L in red for the HOMO and LUMO in green (flipped). Horizontal axis: the index sequence r of AOs ordered along the amino acid sequence. Inset: enlarged part of the box.

$E_i)/(E_{i+k+1} - E_{i-k})$. The choice of k depends on the variability of the density of energy levels. Statistical averaging would require large k values, while fast variation (especially singularities) in the density of energy levels restricts our choice to low values. We have found that a choice of $k = 2 \ldots 5$ ensures the stability of the distribution in our examples. Next, following standard procedures[31], the cummulative spacing $I(S) = \#\{s_i < S\}/N = \int_0^S P(s)ds$ is calculated and compared to the theoretical predictions. For the Poissonian statistics $I_P(S) = 1 - \exp(-S)$, for the Wigner surmise $I_W(S) = 1 - \exp(-\pi S^2/4)$ and for the semi-Poissonian transitional statistics $I_{SP}(S) = 1-(2S+1)\exp(-2S)$. In the main part of Fig. 3. we show the cummulative level spacing for the 6328 spacings in the spectrum of Myoglobin and in the inset we show the difference to $I_{SP}(S)$. We can see that without any parameter fitting the spacings for Myoglobin follow the critical theoretical curve with astonishing precision. Note, that no parameter fitting is involved in the procedure, the calculated spacing distribution has a less than 3% error like in the case of systems of critical quantum chaos[26, 20], which are purely theoretical models as opposed to our case, where the positions of atoms in the protein are obtained experimentally.

In addition to Myoglobin, we included in Fig. 3. two other proteins with known biochemical functions, selected randomly from the PDB just by size (close to 10000 valence AOs) and by the availability of the necessary structural data including the coordinates of Hydrogen atoms. Human profilin (PDB ID:1PFL)[39] in solution form has $N = 5232$ valence AOs. It is a ubiquitous eukaryotic protein that binds to both cytosolic actin and the phospholipid phosphatidylinositol-4,5-bisphosphate. Human apolipoprotein E (PDB ID:2L7B)[40] has $N = 11980$ valence AOs. It is one of the major determinants in lipid transport, playing a critical role in atherosclerosis and other diseases. One can see that these other randomly picked proteins are also on the critical curve with the same precision as Myoglobin. Further analysis (not shown here) reveals essentially the same $D_2 \approx 0.5$ values and the same generalized dimension D_q

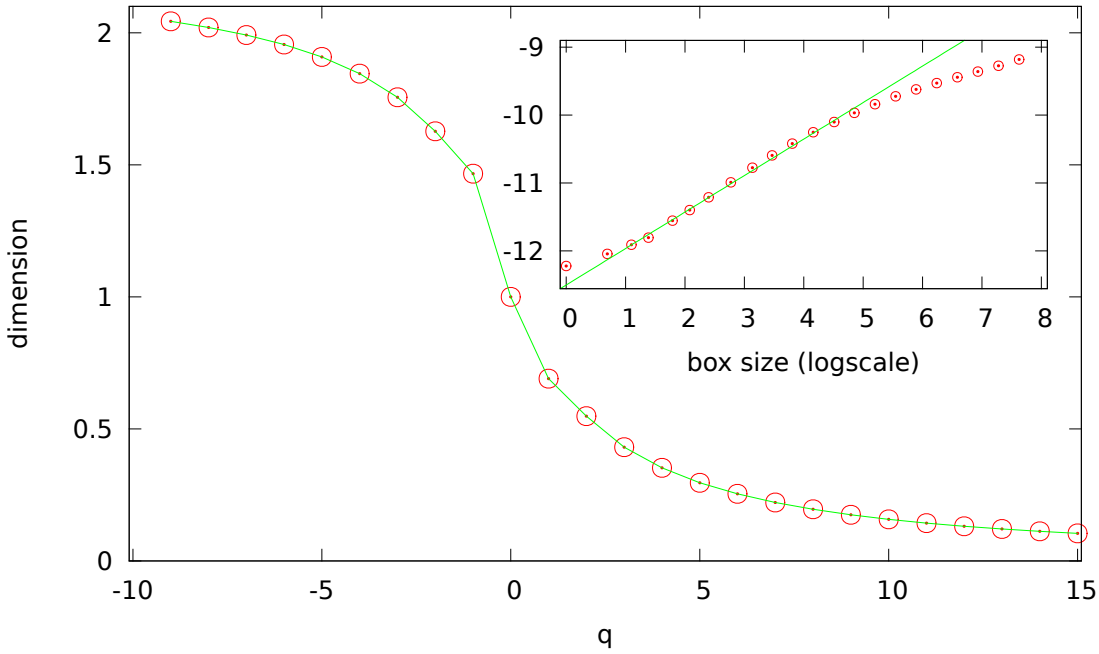

Figure 2. Generalized fractal dimensions D_q of wave functions of the protein Myoglobin (PDB ID:1MYF) averaged for all energies from the Extended Hückel calculation. Inset: Scaling of χ_q for $q = 2$ as a function of the box length l on a double logarithmic plot. The green linear function is fitted to the scaling region and its slope yields the correlation dimension $D_2 = 0.5 \pm 0.01$.

spectra for these proteins as well.

We should emphasize again, that finding a large tight binding Hamiltonian tuned exactly or almost exactly to the critical point by random chance can happen only with an astronomically low probability. So, finding just a single protein with more than 100 amino acids having this property at random is impossible.

Next, we investigate whether criticality is restricted to certain proteins only or is it a more wide spread phenomenon. The verification of fractality is not possible for smaller molecules as it requires a length scale of two decades (say $l \sim 10 - 1000$) to fit a reliable power law to the curve $\chi_q(l) \sim l^{\tau(q)}$. In the case of level statistics we need much less data to verify the shape of the cumulative level spacing $I(S)$. In the RMT analysis in solid state physics and quantum chaos normally on the order of a thousand levels is sufficient. Here we have found that using the technique developed for smaller data sets and the usage of cumulative level statistics $I(S)$ instead of the distribution function $P(s)$, which requires the binning of the data, jointly allow us to verify molecules with as low as $N = 80$ valence AOs reliably. In Fig. 4. we show a collection of level statistics coming from organic molecules of various size. The 3D structures of small molecules were taken from PubChem[41] and the energies are calculated with the EH method (YAeHMOP).

Our first and most striking observation is that each molecule investigated from the biological domain belongs to one of the "clean" categories I_P, I_W or I_{SP}. The reason is by no means obvious. In RMT[24] and especially in quantum chaos[42] intermediate distributions between the classes occur in finite systems. It seems that the Hamiltonians of these biomolecules are not random, they are tuned firmly to one of the classes.

Our first example is Silk (PDB ID:1SLK)[43], a protein which serves as a structural material

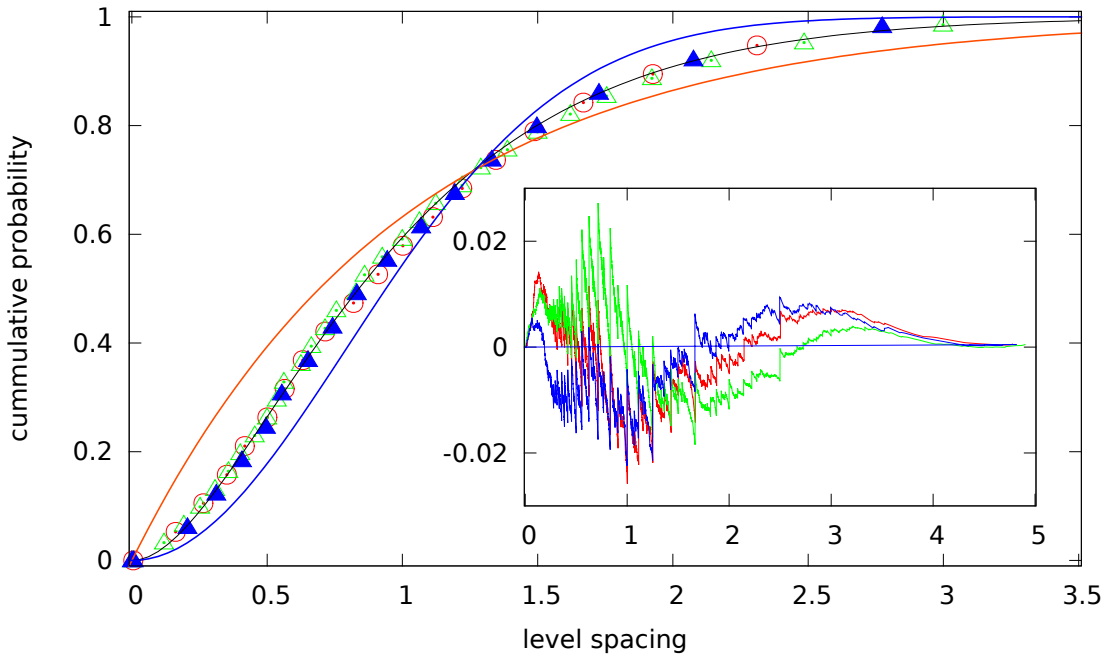

Figure 3. Cummulative level spacing distribution $I(S)$ for Myoglobin (blue triangles), Profilin (red circles) and Human Apolipoprotein E (green circles) are shown. Only every 300 value is shown for legibility. For comparison the theoretical curves $I_P(S)$ (red line), $I_W(S)$ (blue line) and $I_{SP}(S)$ (black line) are also shown. Inset: Difference between the data curves and $I_{SP}(S)$ are shown with the colour of the data set. Each value is plotted. The error is below 3% in probability.

and does not take an active part in biochemical processes. In Fig. 4. we can see that it has Poissonian level statistics and it belongs to the localized class. This is in line with the fact that silk is a very good insulator. This example confirms that criticality is not the property of individual amino acids. Amino acid sequences can produce not just critical materials but insulators as well.

Other examples for structural biomaterials in Fig. 4. are Dextrin (CID 62698), which is a gum like substance and Octadecane (CID 11635) which is an alkane hydrocarbon found in mineral oil and Gefarnate (CID 5282182) a water insoluble terpene fatty acid. They all show Poissonian level statistics and are good insulators.

It is less obvious why DNA belongs to this category. In Fig. 4. we show level statistics for a 21 basis pair DNA sequence (NDB ID:2JYK)[44] which is clearly Poissonian.

The conductivity properties of DNA or RNA sequences are highly debated, however there seems to be a consensus that native DNA is a wide band gap semiconductor, practically an insulator[45].

We picked a few representatives from essential classes of biomolecules. From each class we used the molecule with the largest number of AOs possible among all possible molecules having complete 3D crystallographic data in PubChem. They all show criticality and semi-Poissonian statistics. The list includes Linoleic acid (CID 5280450), Primary fluorescent chlorophyll catabolite (CID 54740347), Sucrose (CID 5988), Vitamin D3 (CID 25245915), Vitamin B12 (CID 16212801) and the largest amino acid Leucine (CID 6106). We investigated a dozen more biomolecules of lesser size. For all practical purposes they all showed semi-Poissonian statistics, but the statistics had larger errors due to the small number of levels. This list includes

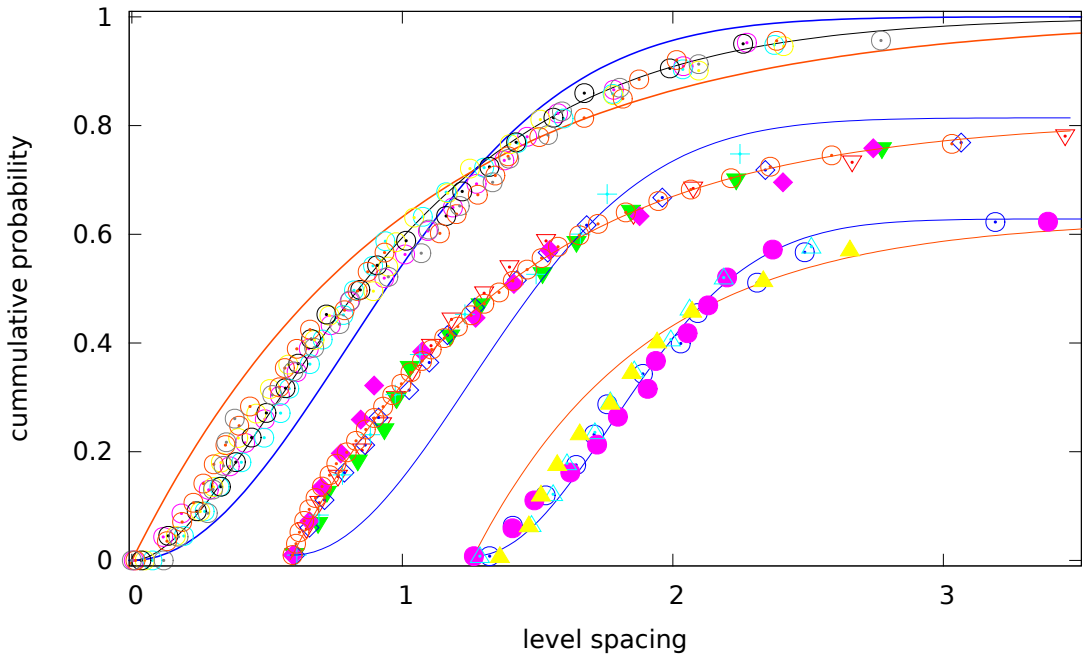

Figure 4. Cummulative level spacing distribution for various molecules. (Only 10-15 data points for each molecule is shown for legibility.) The main part: Molecules with critical cummulative level statistics $I_{SP}(S) = 1-(2S+1)e^{-2S}$. The molecules shown are Vitamin B12, Vitamin D3, Linoleic Acid, Primary fluorescent chlorophyll catabolite, Sucrose and Leucine. Middle part: Molecules with Poissonian cummulative level statistics $I_P(S) = 1-e^{-S}$ (Notice, that the inset is zoomed and the main axis scales don't apply). The molecules shown are Dextrin, Silk, Octadecane, Gefarnate and a 21 base pair DNA sequence (NDB ID: 2JYK). Small part: Molecules with Wigner cummulative level statistics $I_W(S) = 1-e^{-\pi S^2/4}$ (Notice, that the inset is zoomed and the main axis scales don't apply). The molecules shown are Testosterone, Progesterone, Dibenzo(a,e)pyrene and Aristolochic Acid.

Nicotine, Adenosine, Caffeine, Amphetamine, Benzoanthracene, Chlorpozamine, Glucose, Fatty acids omega 3 and omega 6, Picrotin, Picrotoxin, Theophylline, Thiactin, Xanthine. We also carried out the analysis for the 20 amino acids coded by the universal genetic code. They are generally too small for the analysis of the level statistics to the level shown in Fig. 4. but some of them can already be classified by inspection. Based on this it is likely that Arginine, Cysteine, Sele Histidine, Isoleucine, Leucine, Methionine, Phenylalanine, Proline, Serine, Threonine and Tryptophan are critical and Alanine, Asparagine, Aspartic-acid, Glutamic-acid, Lysine, Tyrosine and Valine show Poissonian level statistics. For Glutamine and Glycine the results are inconclusive.

We can also find molecules which belong to the good conductor class with Wigner level spacing statistics. We could find this only in polycyclic molecules with delocalized wave functions spreading through the entire molecule. In Fig. 4. we show Testosterone (CID 6013), Progesterone (CID 5994), Dibenzo(a,e)pyrene (CID 9126) and Aristolochicacid (CID 2236). Among biomolecules we could find only Steroids in this class, the rest of such molecules were involved in combustion such as polycyclic aromatic hydrocarbons and were toxic or carcinogenic.

We can summarize these findings as follows: Most of the molecules taking part actively in biochemical processes are tuned exactly to the transition point and are critical conductors.

There is only the special class of polycyclic molecules with closely packed aromatic rings which show metallic behaviour and delocalization and the class of "structural materials" which play a role in the mechanical stiffness of biological systems. Individual amino acids can be Poissonian or critical but they seem to form proteins and polypeptides which are also either Poissonian or critical.

These findings suggest an entirely new and universal mechanism of conductance in biology very different from the one used in electrical circuits. In metallic conductors charges float due to voltage differences. The electrical field accelerates electrons while scattering on impurities dissipates their energy fixing a constant average propagation velocity. In biological systems we seldom see examples for this. A more likely scenario is that a charge entering a critical conductor biomolecule will be under the joint influence of the quantum Hamiltonian and the excessive decoherence caused by the environment[46]. Such conductance mechanism has been found for the excitons in light harvesting systems[47] and it is currently in the focus of research in Quantum Biology[48]. In these systems Environment-assisted Quantum Transport[49] (ENAQT) is dominant and facilitates the fast quantum spreading of excitations over the system. We think that this mechanism is more universal in biological systems and charges in biological conductors are also subjects of this transport mechanism. Recently we have shown[50] that ENAQT is the most effective at the critical point of the localization-delocalization transition and the excitonic Hamiltonians of light harvesting systems are also at or near the critical point[51]. In the localized regime transport is hindered by strong quantum effects, while in delocalized systems decoherence destroys quantum propagation and the anti-Zeno effect[49] slows down diffusion. At the mobility edge the existence of extended multifractal wave functions throughout the system ensure end-to-end transport while coherence decays only algebraically[50] ensuring a longer coherence time and supressing the anti-Zeno effect.

Our results also suggest that quantum transport played a distinguished role in evolution and selection. Both the number of known small molecules and proteins is about 10^8 and the number of chemically feasible small ($< 500Da$) organic compounds is astronomical, estimated[52] to be 10^{60}. The number of proteins grows exponentially with the number n of amino acids as $\sim 20^n$, and the largest known has about $n \approx 26000$. This shows that chemical and biological evolution selected only a tiny fraction $p \sim 10^{-50}$ of possible small biomolecules and even less for proteins. As the probability of finding a critical molecule or protein by random chance is also astronomically low, the large number of critical molecules and proteins found by quasi random browsing of major databases just by size and availability of the 3D crystallographic data suggests that criticality of the quantum Hamiltonian is prevailing in the evolutionary selection of biomolecules. Besides, the fact that some proteins are natural critical conductors may open up new avenues in materials science as well.

References

[1] Kauffman S A 1993 *The origins of order: Self-organization and selection in evolution* (Oxford Univ. Press)
[2] Crutchfield J P and Young K 1988 *The Santa Fe Institute, Westview* (Citeseer)
[3] Langton C G 1990 *Physica D: Nonlinear Phenomena* **42** 12–37
[4] Maynard Smith J 1995 *The New York review of books* **42** 28–30
[5] Mora T and Bialek W 2011 *Journ. Statist. Phys.* **144** 268–302
[6] Lewin R and Bak P 1993 *Am. Journ. Phys.* **61** 764–765
[7] Bak P, Tang C and Wiesenfeld K 1988 *Phys. Rev. A* **38** 364
[8] Anderson P W 1958 *Phys. Rev.* **109** 1492
[9] MacKinnon A and Kramer B 1981 *Phys. Rev. Lett.* **47** 1546
[10] Wegner F 1981 *Z. Phys. B: Condensed Matter* **44** 9–15
[11] Castellani C and Peliti L 1986 *Journ. Phys. A: Mathematical and General* **19** L429
[12] Evers F and Mirlin A D 2008 *Rev. Mod. Phys.* **80** 1355
[13] Hofstadter D R 1976 *Phys. Rev. B* **14** 2239
[14] Harper P 1955 *Proc. Phys. Soc.: Section A* **68** 879

[15] Aubry S and André G 1980 *Ann. Israel Phys. Soc.* **3** 37
[16] Evangelou S 1990 *Journ. Phys. A: Mathematical and General* **23** L317
[17] Bohigas O, Giannoni M J and Schmit C 1984 *Phys. Rev. Lett.* **52** 1
[18] Berry M V and Tabor M 1977 *Proc. Roy. Soc. London. A. Mathematical and Physical Sciences* **356** 375–394
[19] Richens P J and Berry M V 1981 *Physica D: Nonlinear Phenomena* **2** 495–512
[20] Bogomolny E and Schmit C 2004 *Phys. Rev. Lett.* **92** 244102
[21] Wigner E P 1955 *Ann. Mathematics* **62** 548–564
[22] Dyson F J 1962 *Journ. Math. Phys.* **3** 140–156
[23] Brody T A, Flores J, French J B, Mello P A, Pandey A and Wong S S M 1981 *Rev. Mod. Phys.* **53**(3) 385–479
[24] Guhr T, MuellerGroeling A and Weidenmueller H A 1998 *Phys. Rep.* **299** 189–425
[25] Shklovskii B I, Shapiro B, Sears B R, Lambrianides P and Shore H B 1993 *Phys. Rev. B* **47**(17) 11487–11490
[26] Evangelou S and Pichard J L 2000 *Phys. Rev. Lett.* **84** 1643
[27] Aronov A G, Kravtsov V E and Lerner I V 1994 *JETP Lett.* **59** 40
[28] Aronov A G, Kravtsov V E and Lerner I V 1995 *Phys. Rev. Lett.* **74** 1174
[29] Evangelou S 1994 *Phys. Rev. B* **49** 16805
[30] Varga I, Hofstetter E, Schreiber M and Pipek J 1995 *Phys. Rev. B* **52** 7783
[31] Bogomolny E B, Gerland U and Schmit C 1999 *Phys. Rev. E* **59** R1315
[32] Bogomolny E, Gerland U and Schmit C 2001 *Europ. Phys. Journ. B-Condensed Matter and Complex Systems* **19** 121–132
[33] Hoffmann R 1963 *Journ. Chem. Phys.* **39** 1397–1412
[34] Pople J A and Beveridge D L 1970 *Approximate molecular orbital theory* vol 30 (New York: McGraw-Hill)
[35] Watson H C 1969 *Prog. Stereochem.* **4** 299–333
[36] Ösapay K, Theriault Y, Wright P E and Case D A 1994 *Journ. Molec. Biol.* **244** 183–197
[37] Berman H M, Westbrook J, Feng Z, Gilliland G, Bhat T N, Weissig H, Shindyalov I N and Bourne P E 2000 *Nucleic acids research* **28** 235–242
[38] Schreiber M and Grussbach H 1991 *Phys. Rev. Lett.* **67** 607
[39] Metzler W J, Farmer B T, Constantine K L, Friedrichs M S, Mueller L and Lavoie T 1995 *Protein Science* **4** 450–459
[40] Chen J, Li Q and Wang J 2011 *Proc. Nat. Acad. Sci.* **108** 14813–14818
[41] Bolton E E, Wang Y, Thiessen P A and Bryant S H 2008 *Annual reports in computational chemistry* **4** 217–241
[42] Berry M V and Robnik M 1984 *Journ. Phys. A: Mathematical and General* **17** 2413
[43] Fossey S A, Némethy G, Gibson K D and Scheraga H A 1991 *Biopolymers* **31** 1529–1541
[44] Masliah G, René B, Zargarian L, Fermandjian S and Mauffret O 2008 *Journ. Molec. Biol.* **381** 692–706
[45] Mallajosyula S S and Pati S K 2010 *Journ. Phys. Chem. Lett.* **1** 1881–1894
[46] de la Lande A, Babcock N S, Řezáč J, Lévy B, Sanders B C and Salahub D R 2012 *Phys. Chem. Chem. Phys.* **14** 5902–5918
[47] Engel G S, Calhoun T R, Read E L, Ahn T K, Mančal T, Cheng Y C, Blankenship R E and Fleming G R 2007 *Nature* **446** 782–786
[48] Huelga S F and Plenio M B *Nature Physics* **10** 621–622
[49] Rebentrost P, Mohseni M, Kassal I, Lloyd S and Aspuru-Guzik A 2009 *New Journ. Phys.* **11** 033003
[50] Vattay G, Kauffman S and Niiranen S 2014 *PloS one* **9** e89017
[51] Vattay G and Kauffman S A 2013 *Preprint arXiv:1311.4688*
[52] Reymond J L and Awale M 2012 *ACS chemical neuroscience* **3** 649–657